EasyChair Preprint

№ 3513

Reactor Power Level Estimation by Fusing Multi-Modal Sensor Measurements

Nageswara Rao, Christopher Greulich, Satyabrata Sen, Kenneth Dayman, Jason Hite, Will Ray, Richard Hale, Andrew D. Nicholson, Jared Johnson, Riley D. Hunley, Monica Maceira, Chengping Chai, Omar Marcillo, Tom Karnowski and Randall Wetherington

May 30, 2020

Reactor Power Level Estimation by Fusing Multi-Modal Sensor Measurements

Nageswara S. V. Rao*, Christopher Greulich*, Satyabrata Sen*, Kenneth J. Dayman*, Jason Hite*
Will Ray*, Richard Hale*, Andrew D. Nicholson*, Jared Johnson*, Riley D. Hunley*,
Monica Maceira*, Chengping Chai*, Omar Marcillo†, Tom Karnowski*, Randall Wetherington*
*Oak Ridge National Laboratory, Oak Ridge, Tennessee, USA
Email: raons@ornl.gov
†Los Alamos National Laboratory, Los Alamos, New Mexico, USA

***Abstract*—Estimates of the power level of a nuclear reactor based on measurements from an independent monitoring sensor system can help in the compliance verification of its declared operations. We present a three-level fusion method to estimate the power level of a nuclear reactor using features derived from infrared, electromagnetic, and acoustic sensor measurements collected in proximity to the reactor. Based on a simplified analytical model of the secondary coolant system of the reactor, we identify partial regression functions of the power level in terms of the temperature difference between inlet and outlet of coolant pipes, and the activity levels of four fans and four pumps, which are estimated as features from the sensor measurements. The power level estimator employs a combination of aggregate and complementary fusion steps at three levels to incorporate the multi-modal features in a structure that reflects the secondary cooling system and its partial regression functions. Using the measurements from a test campaign at an operational reactor, we show that this estimator achieves 3.47% or lower root mean square error under 5-fold cross validation. More generally, these results illustrate a progressive reduction in estimation error as additional modalities are appropriately incorporated, and that the fuser outperforms single modality features and their sub-combinations.**

***Index Terms*—reactor facility, power level estimate, multi-sensor fusion, three-level fuser**

I. Introduction

Estimates of the operating power level of a nuclear reactor using measurements from an independent monitoring system of sensors can help to infer deviations from its declared operations. We consider a simplified version of this problem based on measurements from multiple sensors located outside the secondary coolant system (consisting of pumps, fans, and cooling towers) of the High Flux Isotope Reactor (HFIR) at Oak Ridge National Laboratory (ORNL). The heat generated in the reactor core is exchanged between the primary and secondary coolant systems through a heat exchanger, and it is then carried away and dissipated to the environment via four cooling towers. Working in concert, the four fans and four pumps of the secondary coolant system control the coolant flow and heat dissipation rate to maintain a set temperature of the returned coolant water.

A collection of infrared, electromagnetic (EM), and acoustic sensors located outside the reactor facility monitor the secondary coolant system. Their measurements reflect the coolant system variables including the inlet and outlet temperatures of the coolant, and the activity levels of pumps and fans. Infrared imagery is processed to estimate the inlet and outlet temperatures as well as the activity levels of the fans and pumps. Additionally, the activity levels of two of the fans are estimated from EM current clamps, and the combined activity levels of four fans are estimated from acoustic measurements. We address the problem by designing a power level estimator using features derived from measurements collected under a test campaign at HFIR with known power levels. We propose a three-level estimator that employs a combination of aggregate and complementary fusion steps at its levels to incorporate the multi-modal features using a structure that reflects the secondary cooling system and relationships between its system variables expressed as partial regressions.

We utilize a simplified analytical model of the secondary coolant system that relates the reactor power level to the coolant's inlet and outlet temperatures and flow rate. The activity levels of the fans and pumps reflect these variables, which in turn are related to each other via the underlying system physics and design. Their relationships reflect the coolant system structure as well as the sensor measurements and features derived from them using complex codes. In particular, the activities of pumps and fans together reflect the power level in the aggregate, but they are complementary to the difference between the outlet and inlet temperatures which also reflects the power level. The infrared, EM, and acoustic measurements provide complementary feature estimates of the activities of pumps and fans in different ways. We introduce a *conceptualization diagram* that captures various steps from heat generation at the reactor to feature extraction from sensor measurements. We formulate the reactor power level estimation as a regression problem, and present a three-level fuser that exploits the collective and complementary properties of features.

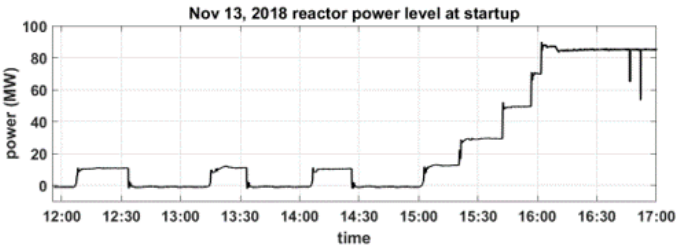

Fig. 1: The power level ground truth during HFIR test campaign.

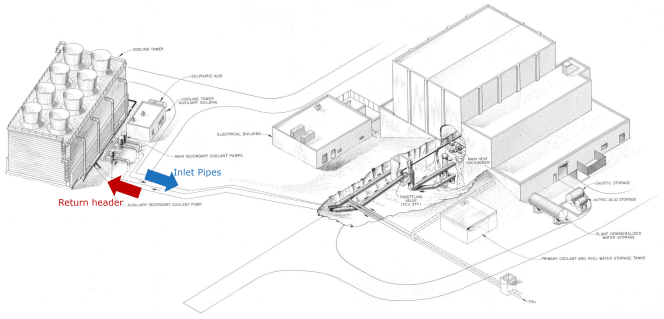

Fig. 2: Secondary coolant system of HFIR.

We use measurements from a test campaign at HFIR under the Multi-Informatics for Nuclear Operations Scenarios (MINOS) venture. Using measurements collected at known power-levels as training data, we demonstrate that a three-level fuser achieves a Root Mean Square (RMS) error of 3.5% under 5-fold cross validation. In addition to fusing features from multiple sensors, the power level estimate is based on fusing four disparate estimators, particularly by combining smooth Gaussian Process Regression (GPR) and Support Vector Machine (SVM) estimates with non-smooth Ensemble of Trees (EOT) and Regression Trees (RT) estimates using a linear fuser (L-F).

We also present power-level estimates using individual sensor modalities and sub-combinations, and the results show a progressive reduction in error as additional modalities are added to the fusion. For example, among single modalities, errors of 16.5% and 5.1% are achieved by EM fan activity estimates and infrared temperature difference estimates, respectively, and the combination of acoustic, EM, and two infrared estimates (temperature difference and fans activity) achieves 4.28% error. Overall, these results illustrate that when appropriately combined, multi-modal fusers achieve performances superior to individual or fewer modalities.

The organization of this paper is as follows. An overview of the HFIR research reactor facility and its secondary coolant system is described in Sections II-A and II-B, respectively. The multi-modal sensors and their measurements are presented in Section II-C. A simplified model of the coolant system and its partial regressions are described in Section III, based on a conceptualization diagram illustrated in Section III-B. Power-level estimation is described in Section IV, including three-level fuser in Section IV-A and estimators using single modalities in Section IV-B. Then, a sequence of fusing individual modalities that illustrates progressive reduction in error is presented in Section IV-C. A summary of contributions and directions for future work are described in Section V.

II. Reactor Facility and Measurements Testbed

To support the development of data analytics for nuclear nonproliferation scenarios, the Department of Energy's (DOE) National Nuclear Security Administration (NNSA) has established the MINOS testbed at ORNL. The testbed is comprised of HFIR outfitted with additional sensors to collect measurements from multiple modalities, including radiation, thermal imagery, seismic, infrasound, electromagnetic, and biological sampling at various distances and locations independent of the main reactor control and monitoring instrumentation. In this paper, we focus on the task of estimating HFIR power level using sensor measurements collected primarily around the reactor's secondary coolant system during a test campaign.

A. High Flux Isotope Reactor

HFIR is a light water research reactor operating at 85 megawatts thermal (MW_{th}), and is used in studies of material irradiation and neutron activation [1], [2]. The typical operating cycle consists of continuous full power operation for around 20 days with start up and shutdown phases each lasting for a few hours. Such operations create unbalanced data sets for estimating intermediate power levels between 0% and 100%, since a majority of the data corresponds to either 0% or 100% power level. To overcome this limitation, a test campaign is designed at HFIR to last for a few hours during which the reactor underwent non-standard power maneuvering to create the training data at different power levels, as shown in Figure 1. The reactor is powered to 10%, held for about 30 minutes, then powered down, and this operation is repeated two more times. Then, the reactor is brought to full power with several incremental stops at intermediate power levels for short periods. Finally, after holding at full power for an hour, the reactor is reduced to 0% power. This process provided a more balanced data set, and the short duration helped to reduce the variability from sensor drifts and/or periodic variations that may occur over the full cycle or multiple cycles.

B. Secondary Coolant System

The heat generated from fission in the HFIR core is carried away by the primary coolant loop and subsequently transferred to the secondary coolant system through a heat exchanger, as shown in Figure 2. The flow rate through the primary loop is approximately 16,000 gpm [1]. The transferred heat is then carried away by the secondary coolant system via the outlet pipe and dissipated by the cooling towers, and the primary coolant is returned to the core at a lower temperature via the cool side. The secondary coolant system consists of four pumps that circulate the water through four cooling towers. Each tower has an induced draft counter-flow design with a fan which dissipates the heat to the environment. The secondary

coolant system is designed and controlled to return the coolant in the primary loop at 120 °F [1].

The design of the coolant system does not evenly distribute the thermal load across the four pumps and fans. There are several pump configurations which operate differently according to the reactor state: Two pumps are designated as primary and run continuously during reactor operations; the auxiliary pump runs as needed during operations and serves as a backup in case one of the primary pumps needs to be serviced during operation; and a smaller shutdown and emergency cooling pump runs mainly when the reactor is powered down or during emergencies as the pump can be powered by an on site diesel generator. Additionally, two of the fans are variable speed drives whereas the other two operate at fixed speeds.

C. Multi-Modal Measurements and Features

The sensors used in this study measure a diverse set of signals with varying sampling rates, sensor resolution, and data storage requirements. These measurements are processed to estimate the features including inlet and outlet coolant temperatures and the activity levels of pumps and fans.

1) Infrared Sensors and Features Extracted: FLIR Ax8 thermal imaging sensors are used to monitor the outer surface temperatures of components of the heat exchange system including pipes and pumps. It features an 80 by 60 pixel thermal sensor taking radiometric images at a 1/3-Hz sampling rate. This image is then further masked to isolate specific components within the field of view. The relative temperature difference between various portions of the captured scene is used as an indication of equipment activity. Certain temperature differences provide quantitative state information such as the difference between pixels corresponding to the inlet and outlet pipes (i.e. the hot and cold legs). Other differentials are used as a qualitative indication of activity such as operation of certain pumps and fans.

2) Acoustic Sensors: Three Inter Mountain Labs (IML) Mode SS infrasound sensors in a triangular formation are used. Their analog output is processed by VReftek digitizer (RT130, Trimble) for A/D conversion at 200 samples per second [3]. The total amplitude of the acoustic signal is used as acoustic feature of the aggregated fan activity by integrating the Fourier spectra over 10 seconds time window.

3) Electromagnetic Current Clamps: A series of Schweitzer 5A2000D60 split-core current transformers are used with Pearson 411C current monitors to monitor the electromagnetic signals from power-lines to the facility. The system takes measurements at 200 kHz [4]. These measurements are processed to generate activity level estimates of two fans of the secondary coolant system.

III. Conceptualization Diagram and Partial Regressions

The features extracted from multi-modal sensor measurements are used as inputs to a power-level estimation function, which is identified using a simplified model of the thermal hydraulics of the secondary coolant system, as described in Section III-A. These estimated features are related to the reactor power level via a sequence of steps from heat transfer to measurements to feature extraction, which are captured using a conceptualization diagram that leads to an underlying regression formulation, as described next in Section III-B.

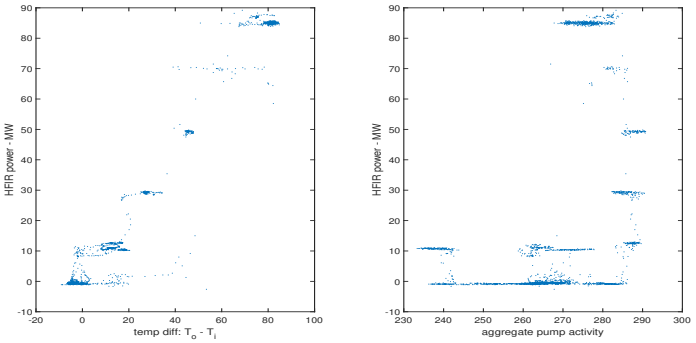

Fig. 3: Variations of HFIR power level with respect to temperature difference (left) and aggregated pump activity (right).

A. Simplified Analytical Model

The reactor operating power-level corresponds to the heat transfer rate $\frac{dQ}{dt}$ reflected in the coolant flow rate $\frac{dm}{dt}$ and in the difference between inlet and outlet coolant temperatures, denoted by T_i and T_o, respectively. Under steady state heat transfer conditions, ignoring the effects of the complex control system and disregarding losses through the heat exchangers, Newton's law of cooling relates these quantities as follows

$$\frac{dQ}{dt} = h\left(\frac{dm}{dt}, c, L, T_\infty\right) A\,(T_o - T_i) \approx B\frac{dm}{dt}(T_o - T_i), \tag{1}$$

where h is the heat transfer coefficient function that depends on several quantities, including the coolant flow rate $\frac{dm}{dt}$, specific heat of the fluid c, characteristic length L, temperature of the bulk liquid T_∞, and others. Also, here A is the surface area of heat transfer, and the outlet temperature T_o corresponds to the hot side of coolant, namely, that leaves the heat exchanger, and the inlet temperature T_i corresponds to the returned fluid after being cooled by the complex of four cooling towers and fans. The return temperature T_i is maintained at a fixed level by the combined flow rate controlled by pumps and heat dissipation at cooling towers controlled by fans. The reactor typically operates at steady state with time-varying but stable plant variables, including $\frac{dm}{dt}$, T_i and T_o. The heat transfer parameters, including c, A and L, are fixed by the design and construction depending on system features including type and length of piping, water pressure, and coolant properties. Thus, the bulk of heat transfer rate is reflected in $\frac{dm}{dt}$, and hence Newton's law of cooling in Equation (1) can be approximated using a constant B (that reflects the plant's design) and the mass flow rate times the temperature difference.

In the simplified Equation (1), power level is linear in the mass flow rate which is reflected in the activity levels of the pumps and fans. These activity levels in turn are captured by the corresponding multi-modal features extracted

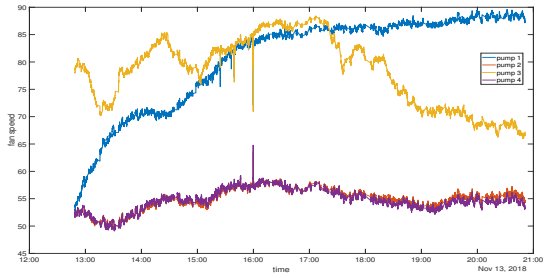

(a) infrared features: pumps 1, 2, 3, and 4

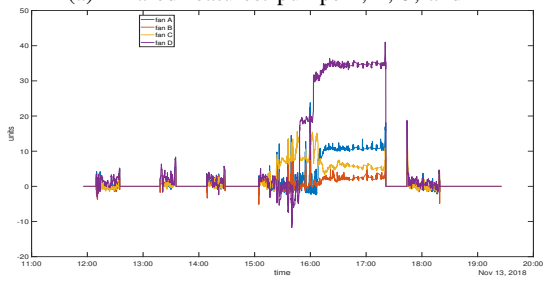

(b) infrared features: fans A, B, C, and D

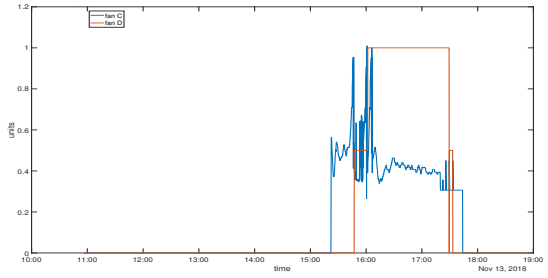

(c) EM features: fans C and D

Fig. 4: Features extracted from measurements variously represent activities of pumps and fans.

from infrared, acoustic, and EM measurements. Overall, the power level is monotonically related to the coolant flow rate, since higher water flow in the cooling towers represents higher heat transfer. Similarly, the power level is also overall monotonically related to $T_o - T_i$ since the return temperature T_i is maintained at a fixed level and a higher power-level results in higher T_o. However, this overall monotonic relationship shown in Figure 3 is complicated by the significant variations in $T_o - T_i$ at each power level.

The pumps operate in a more complex way: two of them come on at a certain power level and operate continuously, while the other two operate as needed such that T_i is maintained at a fixed level. Thus, a monotonic relationship does not hold between individual pump activity levels and the power level; for example, as indicated in Figure 4a, the activity level of pump 3 decreases as HFIR power level is ramped up. The fans show increased activity levels with power level as indicated via infrared features in Figure 4b, however only higher levels of fans C and D are indicated by EM features in Figure 4c. In summary, all pumps and fans operate in concert to dissipate the heat, and hence their aggregated activity level has an overall monotonic relationship with the flow rate, which

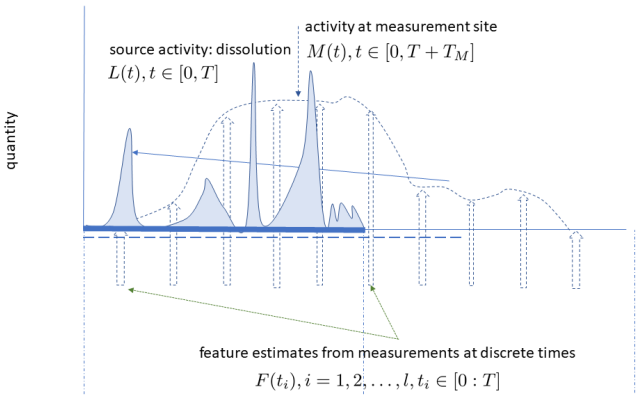

Fig. 5: Conceptual diagram illustrating the steps involved from heat generation to feature extraction.

is exploited in the fuser design presented in Section IV-A.

B. Conceptualization Diagram

The physics of heat transfer and design of the secondary coolant system determine the values of its variables. Additionally, the corresponding extracted multi-modal features reflect the artifacts of sensor measurements and estimator software. The overall effect of various steps leading to feature estimates can be visualized using a conceptualization diagram shown in Figure 5 for a single feature. The solid line $L(t)$ represents the power level that corresponds to power generated at the reactor core. The dotted line $M(t)$ represents the "effective" power level as measured by a sensor at its location, such as T_o or activity level of pump or fan. The measurements and features extracted from them may not necessarily exactly match the qualitative or quantitative aspects of the power level. In addition, the measurement and feature estimation processes discretize the continuous plant variable at the sensor sampling rate. Considering in total l discrete time instants $t_i, i = 1, 2, \ldots, l$, sensor measurements are collected at these instants and are used to estimate a feature $F(t_i)$, which is related to $L(t)$ for some $t \leq t_i$. The power level estimation process can be viewed as "inverting" N estimated features $F_k^{A_k}(t_i), k = 1, 2, \ldots, N$, to generate an estimate $\hat{L}(t_i)$, where A_k is the sensor modality. Under simplified steady state conditions, we consider $\hat{L}(t_i)$ to be an estimate of $L(t_i)$, $t \leq t_i$. Thus, $\hat{L}(.)$ can be viewed as a regression function representing the power level with N estimated features as the independent variables. It is computed using a data set

$$\left\langle (F_1^{A_1}(t_j), F_2^{A_2}(t_j), \ldots, F_N^{A_N}(t_j)); L(t_j) \right\rangle, j = 1, 2, ..., l$$

obtained using measurements collected under a test campaign with known power levels $L(t_j), j = 1, 2, ..., l$.

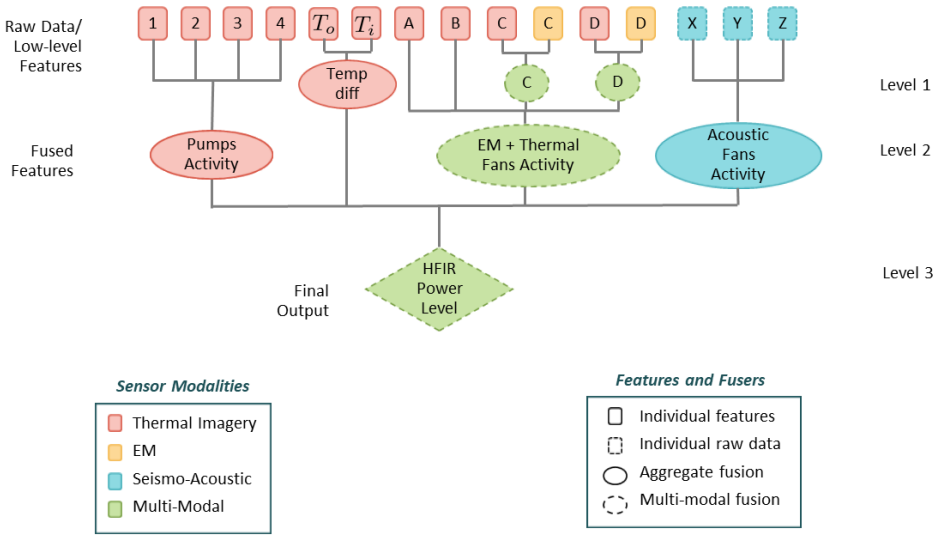

Fig. 6: Three-level fuser consists of complementary, aggregate and complementary fusion steps at level 1, 2, and 3, respectively.

C. Partial Regressions

The activity levels of four fans are represented by f_A, f_B, f_C, and f_D, and the activities of the four pumps are represented by p_1, p_2, p_3, and p_4. The acoustic activity levels at three sensors are represented by a_1, a_2, and a_3. Let us consider the weighted averages of pump and fan activities, respectively denoted by $\bar{p} = \sum_{i=1}^{4} w_i^p p_i$ and $\bar{f} = \sum_{a=A,B,C,D} w_a^f f_a$, as two different estimates of $\frac{dm}{dt}$. Then, using $L(t) - B\frac{dm}{dt}\left(T_o(t) - T_i(t)\right) = 0$ as a simplified version of Equation (1), we have an idealized law that relates the feature variables to power level as

$$2L(t) - B\left(\bar{f}(t) + \bar{p}(t)\right)\left(T_o(t) - T_i(t)\right) = 0. \qquad (2)$$

This is a coarse approximation that captures the relationships between the variables and the power level can also be viewed in terms of partial regression functions. Specifically, using Equation (2), the following partial regression functions of the power level can be identified in terms of:

- inlet and outlet temperatures as $L = R_T\left(T_o, T_i\right)$;
- fan activity levels as $L = R_F\left(f_A, f_B, f_C, f_D\right)$; and
- pump activity levels as $L = R_P\left(p_1, p_2, p_3, p_4\right)$.

Due to the inertial constraints of coolant fluid dynamics, the rate of change of these variables is bounded, which in turn implies that their mutual derivatives are bounded; this condition in turn leads to the smoothness properties of their regressions resulting in a bounded Lipschitz constant. At a more fundamental level, this boundedness property satisfies one of the requirements for the problem of power level regression to be learnable and hence it is solvable using machine learning methods [5]. This bound provides a sufficiency condition for the existence of the generalization equations [5], [6] that quantify how well machine learning methods perform on test data, that is beyond the training set.

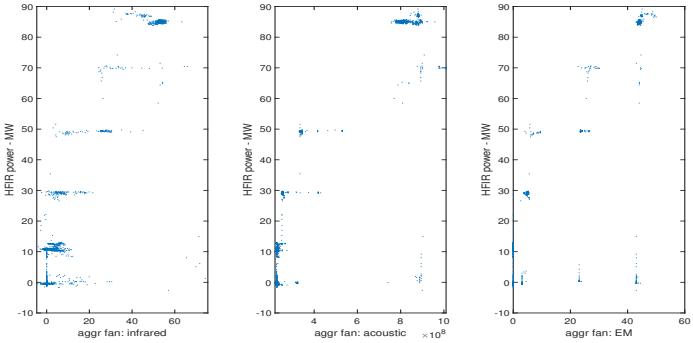

Fig. 7: Power level increases overall with aggregate fan activity infrared (right), acoustic (middle) and EM (right), which all show significant variations.

The features estimated from sensor measurements map to the power level in different ways via the corresponding partial regressions determined from the data sets. The partial regression $L = R_T\left(T_o, T_i\right)$ based infrared features reflected in the left scatter plot in Figure 3 shows an overall increasing trend with significant variations. Such an increasing trend is not evident from the individual pump features p_1, p_2, p_3, p_4, as shown in Figure 4a. However, the right scatter plot in Figure 3 indicates an overall increasing partial regression function $L = R_P(p_1, p_2, p_3, p_4)$ based on aggregate pump activity captured via infrared sensor. The fan features, f_A, f_B, f_C, f_D, estimated from infrared measurements in Figure 4b show even more fluctuation in the start up region. However, the left scatter plot of Figure 7 indicates an increasing partial regression function $L = R_F\left(f_A, f_B, f_C, f_D\right)$ based on aggregate infrared fan activity. Similarly, the middle and right scatter plots of Figure 7 indicate overall increasing

TABLE I: List of sensor modalities, variables, and feature estimates.

Modality	Variable	Feature
infrared	inlet and outlet temperature	T_i^I, T_o^I
infrared	individual pump activity	$p_1^I, p_2^I, p_3^I, p_4^I$
acoustic	aggregated fan activity	f_X^A, f_Y^A, f_Z^A
infrared	individual fan activity	$f_A^I, f_B^I, f_C^I, f_D^I$
EM	individual fan activity	f_C^E, f_D^E

partial regression functions $L = R_F(f_A, f_B, f_C, f_D)$ based on aggregate acoustic fan activity and EM aggregate activity of fans C and D, respectively. In these partial regression functions, there are overall increasing trends between the aggregated activity levels and the power level, but there are also significant variations, which are somewhat smoothed by the corresponding partial regressions. The fusion steps of a three-level estimator further reduces them, leading to a more pronounced monotonic behavior as will be described in the next section.

IV. Power-Level Estimation

Power level estimate is generated by fusing the multi-modal features in a three-level hierarchy that reflects both the physical structure of the coolant system and the partial regressions described in the previous section. The estimator is presented using measurements from the test campaign, which are also used to compute its 5-fold cross validation error to assess its performance. More generally, the test campaign measurements are used to illustrate benefits of multi-modal fusion by comparing with single modality estimates (Section IV-B), and a progressive improvement with additional modalities (Section IV-C).

A. Multi-Modal Features and Three-level Fuser

The multi-modal features of the secondary coolant system are used in complementary, aggregate, and complementary fusion steps at the nodes in three-level hierarchy, as shown in Figure 6. The relationships between the power level and various feature estimates are used in identifying the fusion steps at the nodes as follows:

(a) *Level 3 Complementary Fusion:* The temperature difference and aggregated activities of fans and pumps constitute complementary estimates of the power level. These estimates from level 2 are fused in a complementary fusion step at level 3. They originate from different sensor modality estimates and have different scales, and are fused using non-linear regression and linear fusion methods described later in detail.

(b) *Level 2 Aggregate Fusion:* Three aggregate fusion steps are implemented at level 2 nodes using the activity estimates of pumps and fans based on considerations that reflect their sensor modalities and the coolant system composition. The activity estimates of individual pumps and fans are extracted from the regions of interest in the infrared images. Infrared features for all pumps are linearly fused in the left most level 2 node since they are functionally similar and have the same scale. At the middle level 2 node, infrared features for fans A and B are linearly fused with multi-model estimates of fans C and D from level 1 to obtain the total fan activity estimate based on infrared and EM modalities. Measurements from each of X, Y and Z acoustic sensors reflect the total activity of all fans, and hence their features are linearly fused at right most level 2 node in an aggregation fusion step, since they are located in a close proximity to each other and provide measurements at the same scale.

(c) *Level 1 Complementary Fusion:* Estimates of individual fan activity levels are provided by both infrared and EM features, but the latter only for fans C and D, and hence they are linearly fused using weights chosen to account for their different scales. Also, differences between the outlet and inlet temperatures are computed at this level, which constitute a complementary feature of power level fused at level 3.

TABLE II: Five-fold cross-validation RMS error of the estimators and their fuser.

Method	EOT	GPR	KM	RT	SVM	L-F
RMS error	3.70	3.12	36.41	3.81	3.14	2.95
Percent of peak power	4.36%	3.67%	42.84%	4.48%	3.70%	3.47%

The features estimated using infrared, EM, acoustic, and multi-modal measurements are denoted by superscripts of I, E, A and M, respectively, as indicated in Table I. A generic fusion function R_{1-3}^M that represents the fusion of features at all levels, and its version R_3^M that reflects the three-level fuser are represented using the following expressions:

$$\begin{aligned} L &= R_{1-3}^M\left(p_1^I, p_2^I, p_3^I, p_4^I, T_i^I, T_o^I, \right. \\ &\qquad \left. f_A^I, f_B^I, f_C^I, f_D^I, f_C^E, f_D^E, \right. \\ &\qquad \left. f_X^A, f_Y^A, f_Z^A\right) \\ &= R_3^M\left(\sum_{i=1}^{4} w_i^I p_i^I, \left[T_i^I - T_o^I\right], \right. \\ &\qquad \left. \sum_{a=A,B} w_a^I f_a^I + \left(\sum_{b=C,D}\left(w_b^I f_b^I + w_b^E f_b^E\right)\right), \right. \\ &\qquad \left. \sum_{c=X,Y,Z} w_c^A f_c^A\right). \end{aligned}$$

The fusion function $R_3^M(\cdot)$ represents the complementary fusion step at level 3, and its operands are the results of linear fusion steps at levels 1 and 2.

We obtain an estimate $\hat{R}_3^M(.)$ of $R_3^M(.)$ using the training data from test campaign measurements using five regression estimation methods, namely, EOT, KM, GPR, SVM and RT. As shown in Table II, except KM, both smooth SVM and GPR and non-smooth EOT and RT methods achieve 5-fold cross-validation RMS error under 4.5%, and GPR achieves the lowest error of 3.67%.

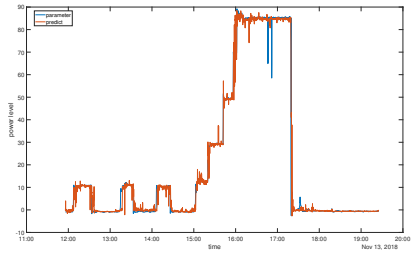

(a) GPR estimate

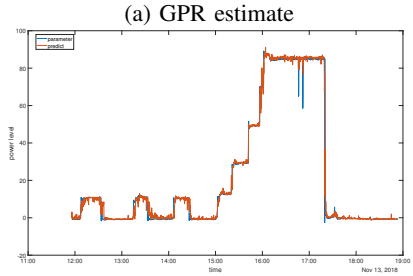

(b) L-F estimate

Fig. 8: Power level estimates of GPR and L-F.

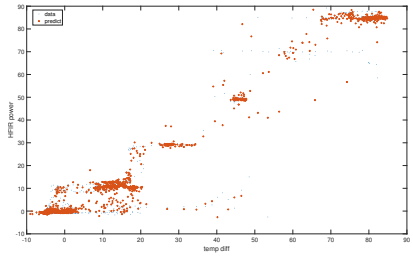

(a) GPR regression

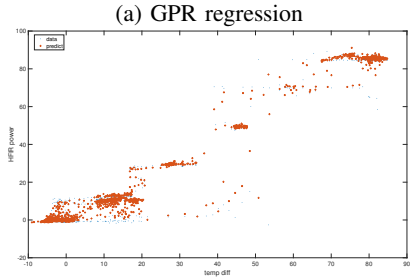

(b) L-F regression

Fig. 9: Partial regressions of power level estimates with respect to temperature difference $T_i - T_o$.

In principle, it is not possible to choose a single universally best method based on a finite number of measurements [7]; this aspect is reflected in part by the closeness of RMS errors in spite of varied nature of the methods, namely, smooth and non-smooth estimates. Instead, we combine the individual estimators using linear fusers (L-F), which results in a further lowering of error to 3.47% while retaining their diversity. The GPR and L-F power level estimates are shown in Figure 8 and their partial regressions with respect to the temperature difference are shown in Figure 9. The fused L-F estimate can be seen as more accurate during the first three 10% power level regions, but the distinction is more subtle in their regressions.

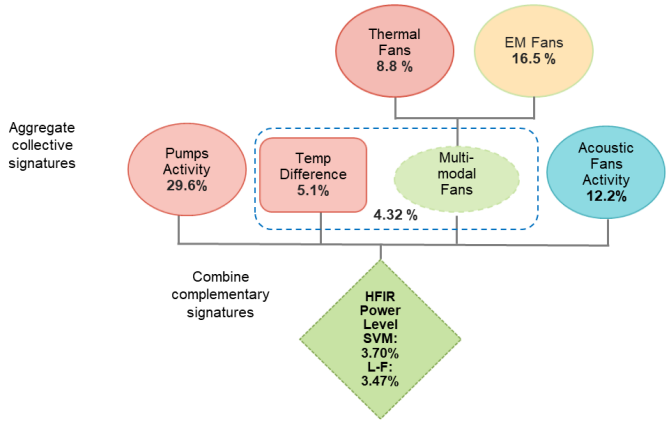

Fig. 10: Error estimates of single and fewer modalities using SVM method.

B. Single Modality Estimators Performance

Errors of single modalities and their sub-combinations are summarized in Figure 10 using the SVM method. The power level estimates based on temperature-difference features, given by $L = R_3^{I:T}\left(T_i^I - T_o^I\right)$, achieves 5.1% error with the SVM method, which is the lowest error among the single modalities. As indicated in Figure 9, there is a significant variation in temperature differences at each power level captured by the regression estimates. The estimate based solely on infrared features of four pumps, given by $L = R_3^{I:P}\left(\sum_{i=1}^4 w_i^I p_i^I\right)$, has 29.6% error, which the highest among single modalities. The estimate based on EM features of fans C and D, given by $L = R_3^E\left(\sum_{b=C,D} w_b^E f_b^E\right)$, has 16.5% error, and that based on infrared features of four fans, given by $L = R_3^{M-F}\left(\sum_{a=A,B,C,D} w_a^I f_a^I\right)$, has 8.8% error. The estimate based on acoustic features, given by $L = R_3^A\left(\sum_{c=X,Y,Z} w_c^A f_c^A\right)$, has 12.2% error which is the third highest among single modalities. Fusion of temperature features with EM and infrared fan features, given by

$$L = R_3^{M:IE}\Big(T_i^I - T_o^I, \sum_{a=A,B} w_a^I f_a^I + \sum_{b=C,D}\left(w_b^I f_b^I + w_b^E f_b^E\right)\Big),$$

has 4.32% error, which is superior to single modalities but still higher than 3.70% of SVM method and 3.47% of L-F method.

C. Progressive Fusion: Performance

To illustrate the effects of fusion of multi-modal features and regression methods, we consider a sequence wherein we progressively add modalities using the SVM method, as shown in Figure 11. We first consider infrared features of temperature and four fans with 4.4% error, which improved over 5.1% compared to the best single modality of the former (shown in top left plot). Then, the addition of EM features of the fans

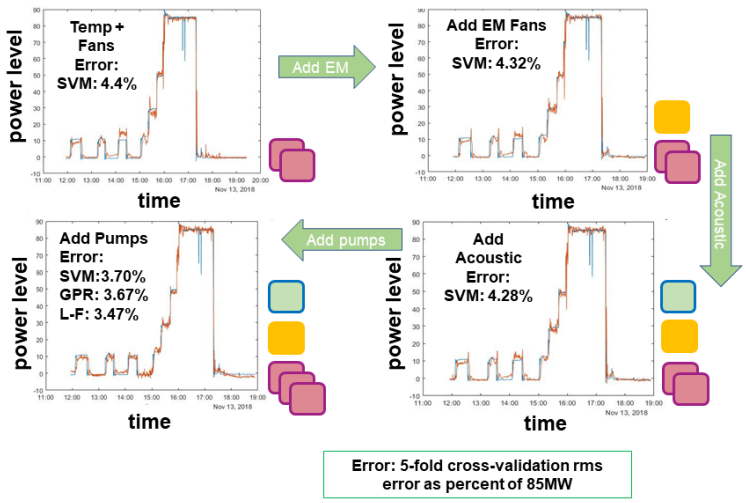

Fig. 11: Illustration of error reduction as different modalities are fused.

C and D leads to a further reduction of error to 4.32% (top right plot). Further addition of acoustic features of the fans reduces the error to 4.28%, which is even further reduced to 3.70% by the 3-level fuser (bottom left plot). Among the individual regression estimates, GPR achieved slightly lower error of 3.67%. Furthermore, in addition to fusing different sensor modality feature, the fusion of four regression methods further reduced the error to 3.47%.

V. Conclusions

This paper is an initial step towards developing analytics for inferring the power level of a nuclear reactor based on independent sensor measurements of its secondary coolant system. Using measurements from a test campaign of an operational reactor, we estimate its power level with 3.47% error by fusing the features derived from infrared, EM, and acoustic measurements. The estimate from a three-level fuser utilizes the temperature estimates of inlet and outlet of the coolant from infrared images, and activity level estimates of the fans from infrared, acoustic, and EM measurements. The fuser employs a combination of aggregate and complementary fusion steps at three levels to incorporate the multi-modal features in a structure that reflects the secondary cooling system and its partial regression functions. This estimate outperforms those based on single modality features and their sub-combinations. More generally, these results illustrate a progressive reduction in estimation error as additional modalities are appropriately incorporated.

It is of future interest to incorporate additional domain specific aspects based on detailed analyses of the primary and secondary coolant systems as well as other reactor subsystems. The results of this paper are based on limited measurements of a single start-up, and it would be important to extend them to more datasets spanning multiple seasons and varied weather conditions. Additional sensor modalities of interest include effluents and radiation measurements collected at the off-gas stack, seismic signals from a variety of sensors, and acoustic signals from orthogonal instruments. Also, the neutrino measurements collected at longer distances from the reactor, and other types of radiation, such as gamma and neutrons, measured in the proximity of reactor would be interesting to consider. It would be of interest to obtain generalization equations of estimators and fusers [8] that provide confidence estimates for the error bounds for future measurements including the ones from other reactors. Further, it would be interesting to provide explanations based on physics and engineering aspects of the reactor that contribute to the power level estimates.

References

[1] ORNL, "High flux isotope reactor (hfir) user guide," tech. rep., Oak Ridge National Lab., Tenn., 2015.

[2] R. Cheverton and T. Sims, "Hfir core nuclear design," tech. rep., Oak Ridge National Lab, 1971. https://doi.org/10.2172/4008514.

[3] C. Ramirez, C. Chai, M. Maceira, and O. Marcillo, "Classification of industrial facility power-levels using seismo-acoustic signatures," in *Proceedings of the INMM 60th Annual Meeting*, vol. 1, pp. 283–293, Institute of Nuclear Materials Management, July 2019.

[4] R. Wetherington, G. Sheets, T. Karnowski, R. Kerekes, M. Vann, M. Moore, and E. Freer, "Novel low-cost approach for acquiring high resolution high-speed data," in *Proceedings of the INMM 60th Annual Meeting*, Institute of Nuclear Materials Management, July 2019.

[5] N. S. V. Rao, "Finite-sample generalization theory for machine learning practice for science," in *DOE ASCR Scientific Machine Learning Workshop*, 2018.

[6] V. N. Vapnik, *Statistical Learning Theory*. New York: John-Wiley and Sons, 1998.

[7] L. Devroye, L. Gyorfi, and G. Lugosi, *A Probabilistic Theory of Pattern Recognition*. Springer-Verlag, New York, 1996.

[8] N. S. V. Rao, N. Imam, Z. Liu, R. Kettimuthu, and I. Foster, "Machine learning methods for connection RTT and loss rate estimation using MPI measurements under random losses," in *International Conference on Machine Learning for Networking*, 2019.